

# Chapter 12

## LEAP-UCD-2017 Centrifuge Tests at Cambridge



Srikanth S. C. Madabhushi, A. Dobrisan, R. Beber, Stuart K. Haigh,  
and Gopal S. P. Madabhushi

**Abstract** As part of the LEAP project the seismic response of a liquefiable 5° slope was modelled at a number of centrifuges around the world. In this paper the two experiments conducted at Cambridge University are discussed. The model preparation is detailed with particular emphasis on the sand pouring, saturation and slope cutting process. The presence of the third harmonic in the input motion is shown and its significance discussed. The potential for wavelet denoising to filter random electrical noise from the pore pressure traces is illustrated. CPT strength profiles are highlighted and a possible softer layer in one of the tests is discussed. Whilst the specifications called for one dense and one loose test, the likelihood that both Cambridge tests were loosely poured is assessed. The PIV technique is used to obtain the displacements of the slope during the test. Finally, the correspondence between the PIV displacements and physical measurements of the marker movements is compared.

### 12.1 Introduction

The great advances in computation power of the last decade have greatly reduced the time and cost barriers of numerically studying highly coupled complex problems such as liquefaction. However, this necessitates high-quality experimental data on liquefaction problems to calibrate and validate the numerical assumptions against. Following in the steps of the VELACS project (Arulanandan and Scott 1993), the Liquefaction Experiments and Analyses Project (LEAP) strives to build a database of reliable centrifuge data from centres around the world to accompany the numerical research. The problem studied in this second phase of LEAP is that of a 5°

---

S. S. C. Madabhushi (✉) · A. Dobrisan · S. K. Haigh · G. S. P. Madabhushi  
Department of Engineering, Cambridge University, Cambridge, UK

R. Beber  
Department of Civil, Environmental and Mechanical Engineering, University of Trento, Trento,  
Italy

liquefiable slope subjected to 1 Hz destructive motions. This paper summarizes the two tests carried out at Cambridge within LEAP. The model preparation at Cambridge follows largely the same procedure originally detailed in the LEAP-GWU-2015 exercise (Madabhushi et al. 2017). In this paper emphasis will be placed on describing the salient differences of the model construction and results with respect to the other centres involved in the project.

## 12.2 Experiment Setup

Two tests were carried out at Cambridge as part of the LEAP 2017 exercise. At prototype scale, both tests modelled a 5° slope of uniform Ottawa F-65 sand, 4 m deep at the midpoint and 20 m in length. Figure 12.1 shows the general test setup, key dimensions and instruments at model scale. A centrifugal acceleration of 40 g at 1/3 the midpoint height was applied in both tests. To investigate the effect of sand density on the dynamic response of the slope, the two Cambridge University LEAP tests (CU01 and CU02) had different prescribed target densities: 1651 and 1599 kg/m<sup>3</sup>, respectively. These corresponded to relative densities of 67% and 48%.

### 12.2.1 Sand Pouring

An automated spot pluviator (Madabhushi et al. 2006) was used for sand pouring. The nozzle aperture (which controls the sand flow rate), drop height and to a less extent the pluviator translation characteristics determine the bulk density of the soil layers poured. This arrangement differs to the LEAP specification in terms of the sieve dimensions and whilst the same range of densities can be obtained the potential for differences in the soil fabric should be borne in mind.

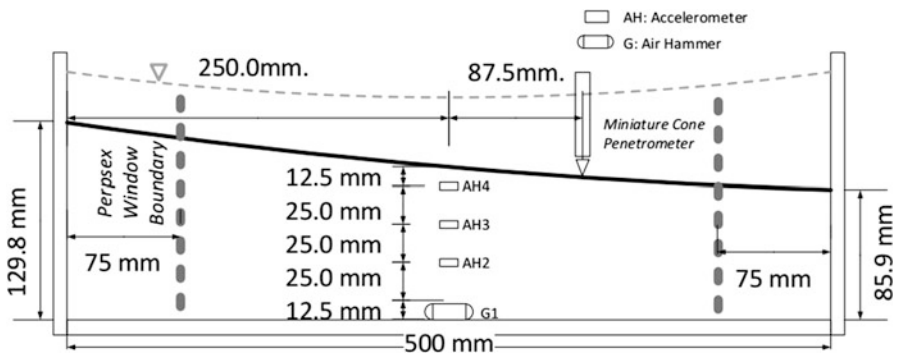
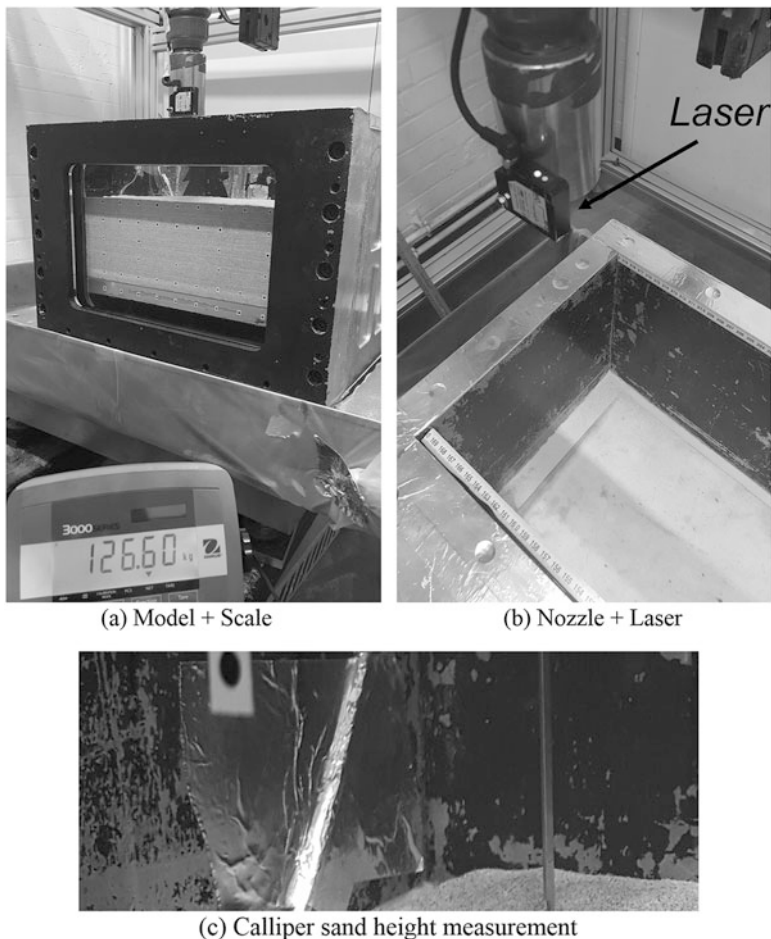


Fig. 12.1 General model schematic—not all sensors shown



**Fig. 12.2** LEAP 2017 sand pouring. (a) Model + scale (b) nozzle + laser (c) calliper sand height measurement

The container was placed on a scale to monitor the sand mass during pluvation without disturbing the model. A laser unit was attached to the hopper nozzle to measure the sand height between the nozzle translations. The height of poured sand was also measured by callipers in conjunction with the laser measurement to increase the number of readings and to check consistency between the two methods of determining height. The pouring setup is presented in Fig. 12.2.

Four calliper measurements were taken for each layer of poured sand. Due to the operation mode of the pluviator, laser measurements could only be taken every fourth layer poured. Figure 12.3a highlights the general agreement between calliper and laser measurements.

Since the sand mass was recorded by the digital scale, the height measurements were used to estimate bulk density. As shown in Fig. 12.3b a relatively small scatter

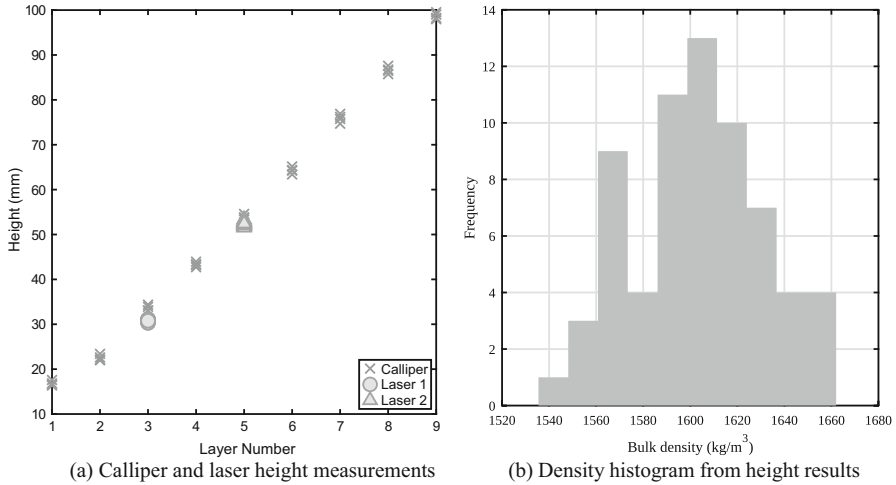


**Fig. 12.3** Comparison of laser and calliper results. Bulk density inference (CU02). (a) Calliper and laser height measurements. (b) Density histogram from height results

**Table 12.1** Mean and standard deviation of bulk density calculations

Test	Target (kg/m <sup>3</sup> )	Mean Achieved (kg/m <sup>3</sup> )	Based on	Standard Deviation (kg/m <sup>3</sup> )
CU01	1652	1630	Trimmed mean of 36 calliper measurements, interior 75 %	43.1
		1656	Trimmed mean of 45 laser measurements, interior 75 %	12.3
CU02	1599	1610	Trimmed mean of 35 calliper measurements, interior 60 %	30.3
		1606	Trimmed mean of 30 calliper measurements, interior 75 %	15

in height measurements translates to rather large uncertainties in density estimation. The same is accentuated in Table 12.1 which includes the standard deviation of the bulk density results.

During pouring instruments were positioned in the sand. An air hammer (Ghosh and Madabhushi 2002) was placed at the base of the model (Fig. 12.4a) in CU02. The impulses it generated, picked up by the piezoelectric accelerometers (Fig. 12.4b), can allow assessment of the shear wave velocity during the test. A list of the sensors employed and their positions can be found in Kutter et al. (2018).

### 12.2.2 Viscosity Measurement

The viscosity of the methyl cellulose used to saturate the model was specified at 40 cSt to fulfil dynamic scaling laws (Schofield 1981). The viscosity was measured

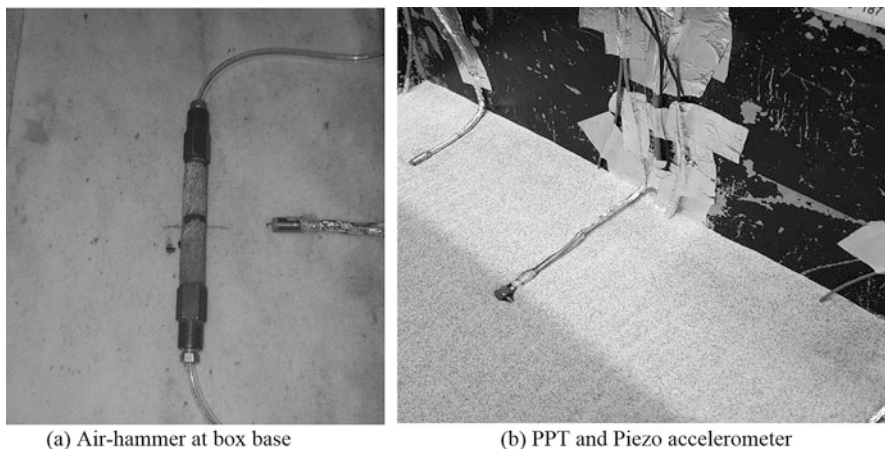


**Fig. 12.4** Instruments in model container (CU02). (a) Air hammer at box base. (b) PPT and piezo accelerometer

**Fig. 12.5** Saturation setup

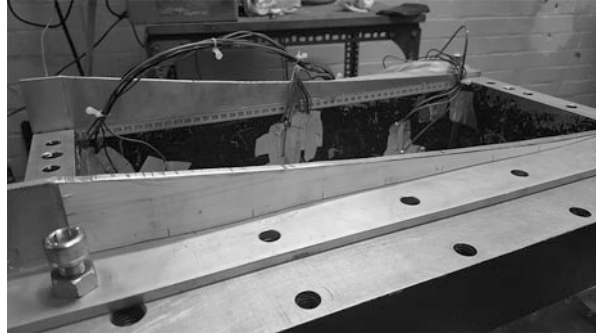


using a viscometer and values from before the test were 45 cSt for CU01 and 44 cSt for CU02. Owing to the temperature dependence of viscosity, the methyl cellulose was prepared with an assumed centrifuge temperature beforehand. A change of 1 °C in the centrifuge yields approximately a 5% difference in viscosity.

### 12.2.3 Saturation

For both tests the models were saturated under vacuum using the CAM-SAT system (Stringer and Madabhushi 2009) that controls the rate of mass influx into the model base (Fig 12.5). A maximum rate of 0.5 kg/h was chosen to prevent fluidization of the soil. Prior to saturation the model was flushed with CO<sub>2</sub> gas in

**Fig. 12.6** Log-spiral guides mounted on top of model container



several cycles to improve the vacuum obtained. However, the degree of saturation could not be accurately determined following the method of Okamura and Soga (2006) due to the measured compliance in the saturation systems tubing. Cross comparison of the excess pore pressure generation between centres can be used to infer the degree of saturation in the Cambridge tests.

### ***12.2.4 Slope Cutting***

After saturation the required slope was cut into a logarithmic spiral shape to accommodate the tangential shaking direction with respect to the package centrifugal motion. A cutting plate running along machined log-spiral guides was used to obtain the desired shape (Fig. 12.6). As discussed in Madabhushi et al. (2017), the fluid level was lowered during the cutting with the resulting capillary suction increasing the effective stress and aiding the shaping process.

In the Cambridge centrifuge the package sits horizontally so the cutting plate was designed to have a 1:40 slope to correct for the angle between the normal  $g$  field and the sand surface. The cut slope is shown in Fig. 12.7.

### ***12.2.5 CPT***

An in-flight CPT mounted on the package (Fig. 12.8) was used to determine soil strength before and after the destructive motion. The CPT used was different to the UC Davis one; however additional centrifuge tests confirmed consistent results between the two devices (Carey et al. 2018).

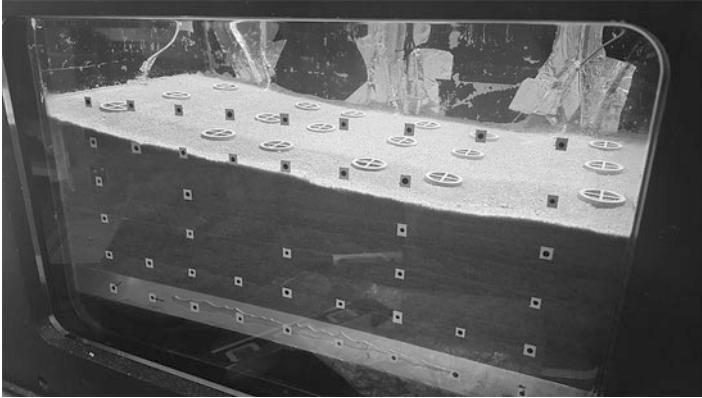
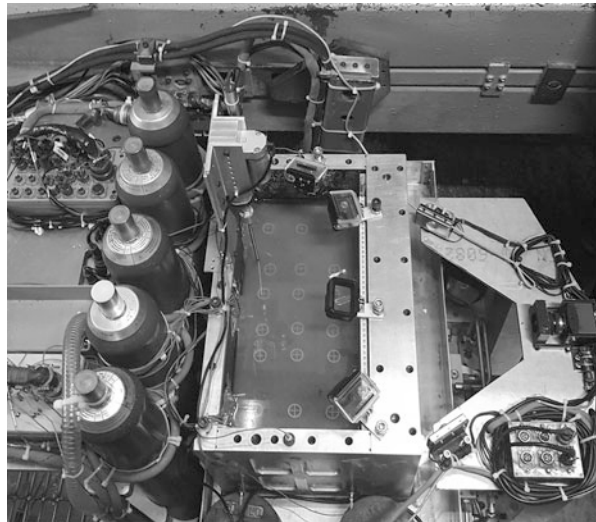


**Fig. 12.7** Cut slope with markers on top

**Fig. 12.8** Centrifuge package with CPT attached



### 12.3 Destructive Motions

The target prototype input motions for both CU01 and CU02 were ramped 1 Hz sines with PGA of 0.15 g. In an attempt to calibrate the desired input motion, dummy packages of the same mass as the actual LEAP models were loaded in an ESB container box (Brennan and Madabhushi 2002) and shaken. As shown in Fig. 12.9, the calibration runs exhibited little high-frequency noise, with most of the shake energy contained within the desired 1 Hz signal.

The recorded input acceleration during the two LEAP tests is shown in Fig. 12.10. As well as the PGA being closer to 0.2 g, the third harmonic at 3 Hz carried

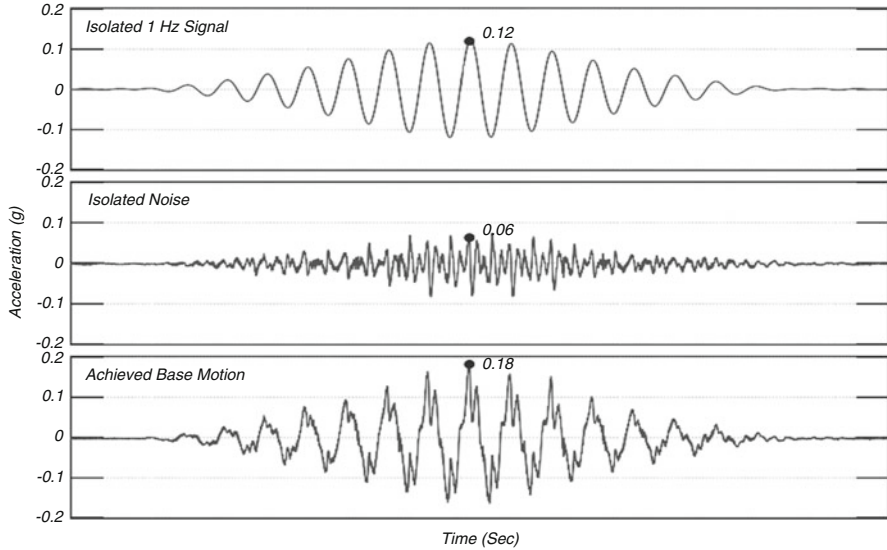


**Fig. 12.9** Input motion and isolated high-frequency component of calibration run

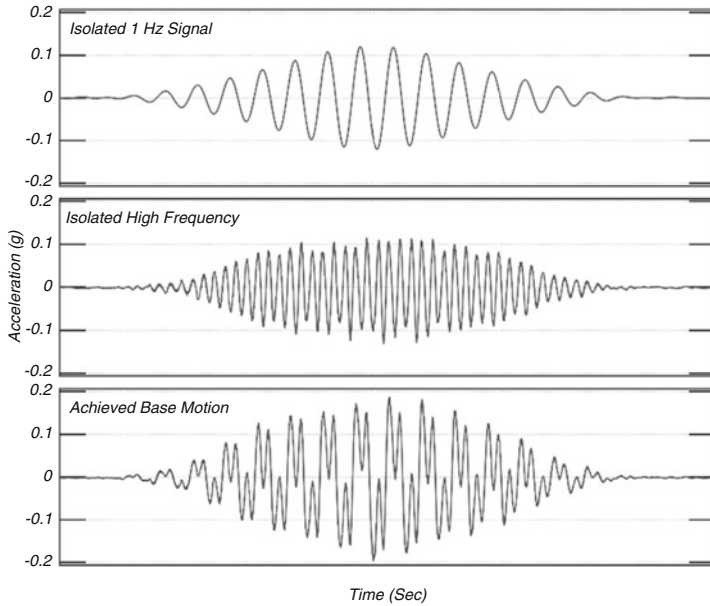
significant energy in both these runs. Although the mass was matched between the LEAP and dummy models, the LEAP tests were carried out in a window box. Potentially, the different box stiffness might have triggered a resonant response of the shaker and model system at 3 Hz. A significant 3 Hz component was also observed previously by Madabhushi et al. (2017) in the LEAP 2015 exercise.

The impact of the third harmonic on the slope behaviour remains an area of research. Comparison between the centrifuge experiments at Cambridge and other centres shows the dilation spikes were less pronounced when compared with tests with a smaller third mode vibration (Fig. 12.11). The attenuated dilation could explain the larger slope displacements recorded during CU01 and CU02 when compared with other centrifuge centres (Fig. 12.12).

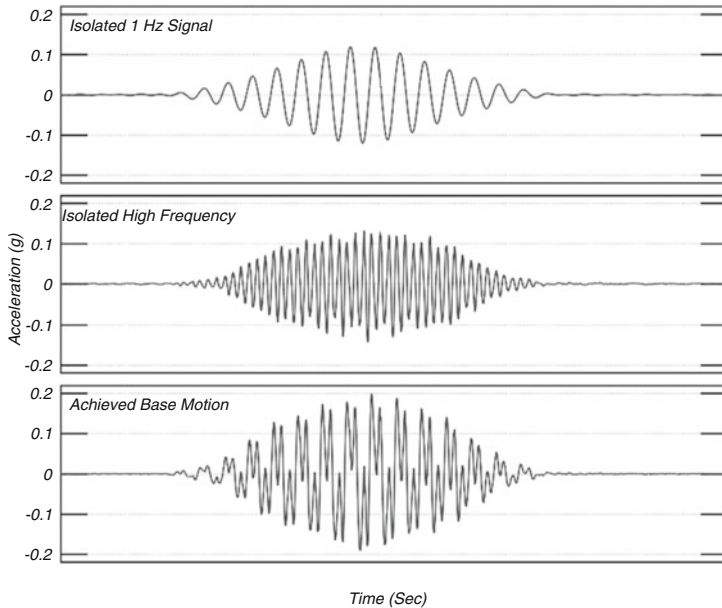
Accurate prediction of the dilation spikes during the slope shaking is numerically challenging. The numerical analyses in Madabhushi et al. (2017) could generally capture the behaviour of the Cambridge centrifuge tests in terms of the accelerations, excess pore pressures and slope displacements. However, the simulations showed little dependence on the third harmonic for the constitutive model and properties used. The potential sensitivity of both the experiments and numerical analyses to the third harmonic requires further comparison and investigation.

The increased noise on six of the eight pore pressure transducers was traced back to a malfunctioning amplifier card. The data presented in Beber et al (2018b) was filtered in the frequency domain using a low-pass filter. The potential for wavelet denoising to better recover the original signal is explored in Fig. 12.13. The relative magnitudes of the real signal and random electrical noise are clearly different and can be easily separated to allow reconstruction of a cleaner signal.





(a) CU01



(b) CU02

**Fig. 12.10** Input motion and isolated high-frequency component. (a) CU01 (b) CU02

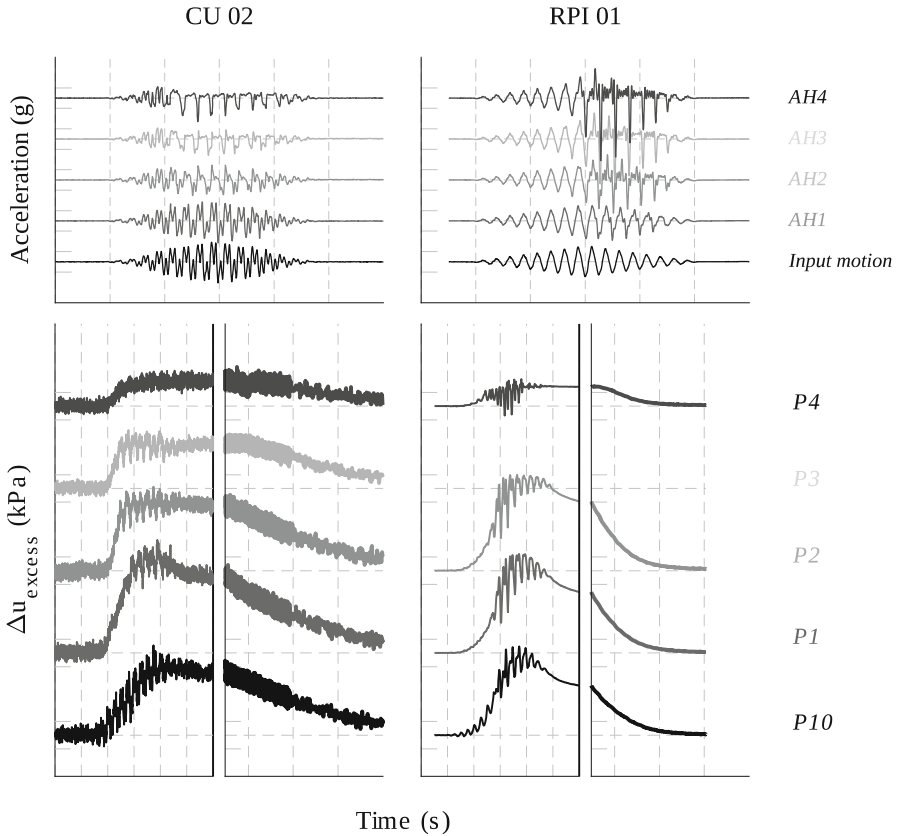


**Fig. 12.11** Presence of significant dilation spikes for input motions with reduced third harmonic

Figure 12.10 highlights the similarity between input accelerations for CU01 and CU02 and Fig. 12.14 shows the associated wavelet-denoised excess pore pressure generation during the two tests. CU01 was designed as a medium dense sand test (Rd 67%) and CU02 as a loose test (Rd 48%). However, the very similar excess pore pressure generation might suggest the difference in density between the two was not as large.

### 12.4 CPT Strength Profiles

The CPT strength traces with depth recorded in-flight before the destructive motion are shown in Fig. 12.15. The CU01 trace suggests a softer sand layer was encountered at 2 m depth. However, given the local nature of a CPT test and the overall consistency of the other instruments in CU01, the “bump” could have been a local effect rather than a general trend.

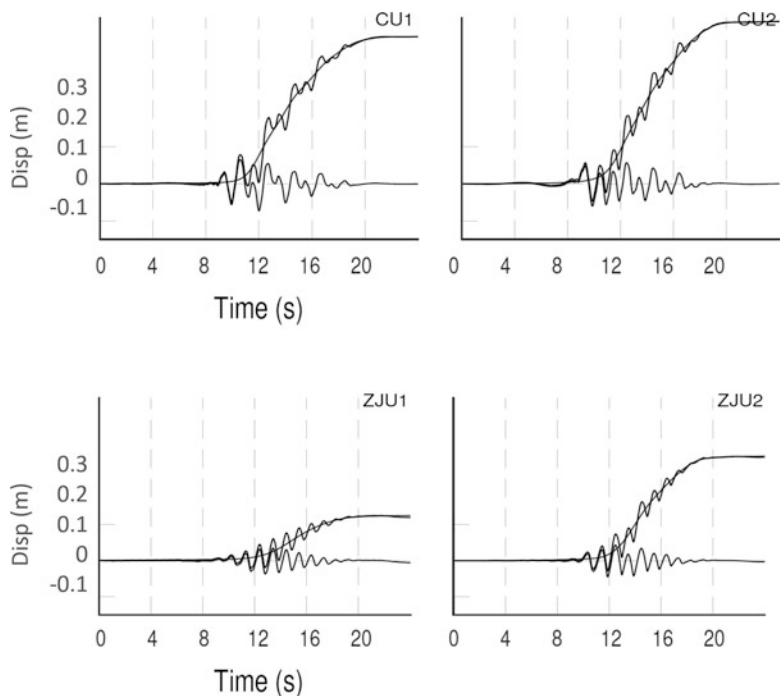


Fig. 12.12 Slope displacement comparison to other test centres

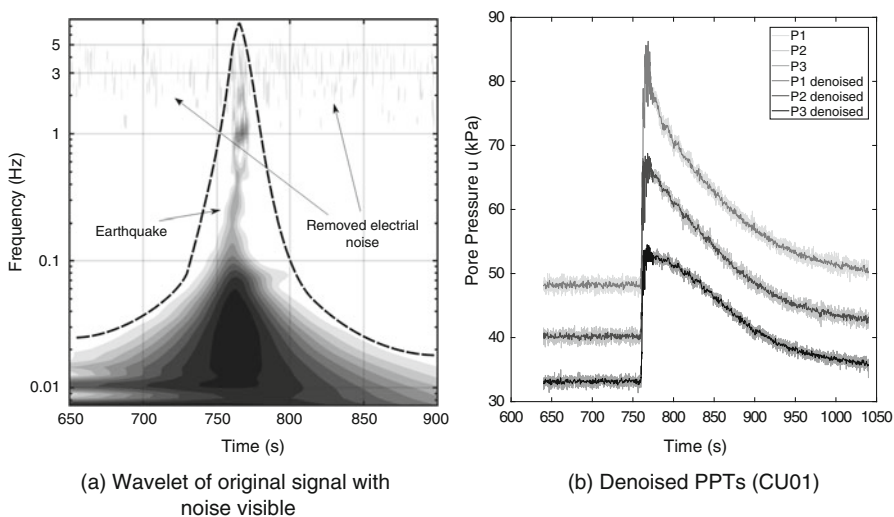


Fig. 12.13 Wavelet denoising. (a) Wavelet of original signal with noise visible. (b) Denoised PPTs (CU01)

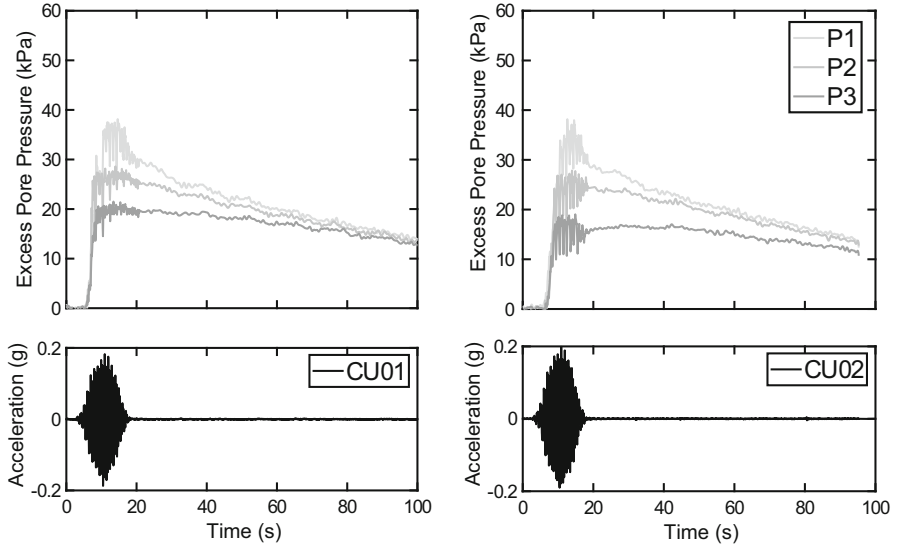
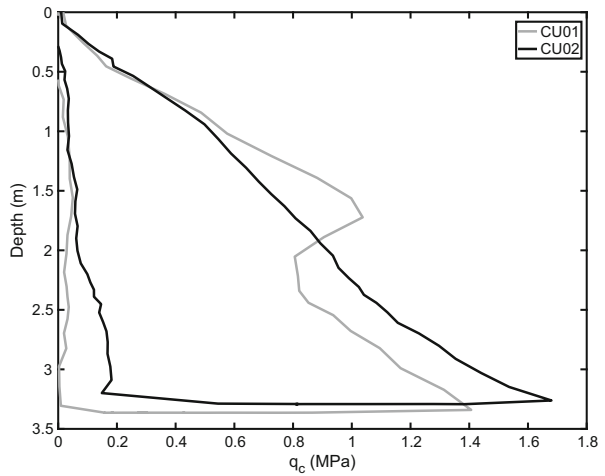


Fig. 12.14 Excess pore pressure generation CU01 and CU02

Fig. 12.15 CPT strength profiles



As shown by Beber et al. (2018a, b), the CPT strength profiles can be correlated with relative density through various empirical correlations. These indicate that CU01 and CU02 have a similarly loose average density.

Comparison of the CPT results between the LEAP 2017 tests reveals other medium-dense tests typically having cone resistances approximately double those recorded in CU01. Overall, caution is recommended if interpreting CU01 as a medium-dense sand test. Nevertheless, the similarity of the accelerations, excess

pore pressure generations, marker displacements and average soil strength between CU01 and CU02 potentially recommend the first test as an additional dataset for a loose sand.

## 12.5 PIV

Images taken during the tests for PIV analysis are available at Beber et al. (2018a, b). These can be used for various analysis scenarios. Beber et al. (2018a, b) show from PIV that soil densification during swing up is small, but not necessarily negligible. Moreover, by tracking soil patches at the same location along the slope as the markers, the consistency between the PIV and marker measurements can be verified. The comparison is shown in Fig. 12.16a, which highlights a considerable difference between the two. As well as the limited measurement precision, the readings may be inaccurate if the markers did not remain fully coupled with the liquefying soil. Equally, the comparison necessitates that the PIV displacements near the Perspex are representative of the slope centreline. The container geometry is detailed by Cilingir and Madabhushi (2010) and may be considered rigid in the plane strain direction.

The dynamic component of the PIV displacement shown in Fig. 12.16b can be extracted. Likewise, the double integral of the accelerometer traces relative to the base motion can give the dynamic displacement of the slope centreline. The comparison between these two methods, shown in Fig. 12.16b, is favourable and suggests the dynamic displacement is fairly uniform across the slope width. This

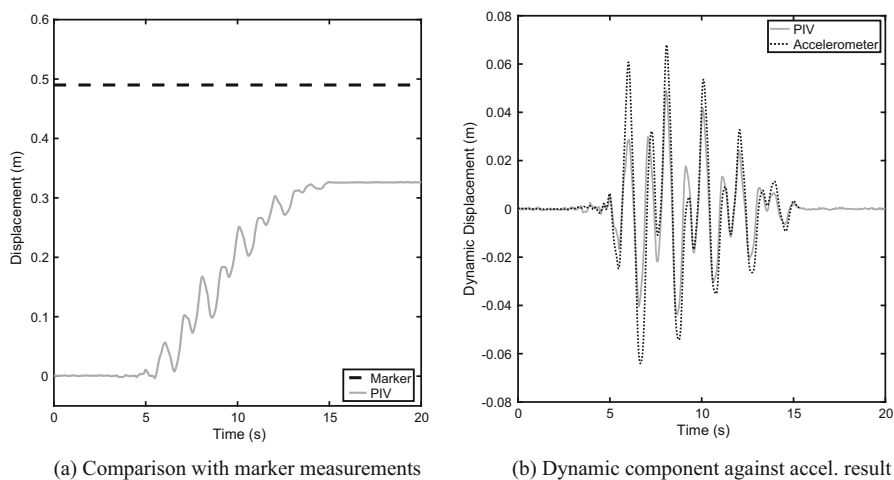


**Fig. 12.16** PIV displacements in CU01. (a) Comparison with marker measurements. (b) Dynamic component against accelerometer result

increases the confidence in the PIV method to accurately determine the total displacement of the slope.

## 12.6 Conclusions

This paper summarized the methodology and results from the LEAP 2017 experiments carried out at Cambridge. The steps taken to measure the mass and height of sand during pouring are shown and the resulting density estimates and their uncertainty highlighted. Cross comparison between the two Cambridge tests, as well as placing them within the wider context of the LEAP database, suggests both CU01 and CU02 had similarly loose initial void ratios. During the tests, the potential for the container dynamics to influence the third harmonic in the input motion is raised, and the implication for the excess pore pressure generation and resulting slope displacement touched upon. The total displacement of the slope can be accurately determined from the PIV method, and the correspondence of the dynamic displacements between the front face and centreline of the slope was assessed. Overall, the importance of thorough examination of the internal consistency of centrifuge data is highlighted, and the value of a large database of results to better understand the relative sensitivity to experimental variations expounded.

**Acknowledgment** The authors wish to express their gratitude to all of the technicians at the Schofield centre for their help and support during the model preparation and testing.

## References

- Arulanandan, K., & Scott, R. F. (1993). *Verification of numerical procedures for the analysis of soil liquefaction problems*. Rotterdam: A.A. Balkema.
- Beber, R., Madabhushi, S. S. C., Dobrisan, A., Haigh, S. K., & Madabhushi, S. P. G. (2018a). LEAP GWU 2017: Investigating different methods for verifying the relative density of a centrifuge model. *International Conference in Physical Modelling in Geotechnics, London*.
- Beber, R., Madabhushi, S. S. C., Dobrisan, A., Haigh, S. K., & Madabhushi, S. P. G. (2018b). CU1, CU2 – University of Cambridge Experiments. In *PRJ-1843: LEAP-UCD-2017*. <https://www.designsafe-ci.org/data/browser/projects/7067616763427688936-242ac11d-0001-012/>
- Brennan, A. J., & Madabhushi, S. P. G. (2002). Design and performance of a new deep model container for dynamic centrifuge testing. In *International Conference on Physical Modelling in Geotechnics* (pp. 183–188). Rotterdam: Balkema.
- Carey, T., Gavras, A., Kutter, B., Haigh, S. K., Madabhushi, S. P. G., Okamura, M., Kim, D. S., Ueda, K., Hung, W.-Y., Zhou, Y.-G., Liu, K., Chen, Y.-M., Zeghal, M., Abdoun, T., Escoffier, S., & Manzari, M. (2019). A new shared miniature cone penetrometer for centrifuge testing. In *Proceedings of 9th International Conference on Physical Modelling in Geotechnics, ICPMG 2018* (Vol. 1, pp. 293–229). London: CRC Press/Balkema.
- Cilingir, U., & Madabhushi, S. P. G. (2010). Particle image velocimetry analysis in dynamic centrifuge tests. In *Proceedings of the 7th International Conference on Physical Modelling in Geotechnics (ICPMG)* (pp. 319–324). Zurich: CRC Press.

- Ghosh, B., & Madabhushi, S. P. G. (2002). An efficient tool for measuring shear wave velocity in the centrifuge. In *Proceedings of the International Conference on Physical Modelling in Geotechnics* (pp. 119–124). Rotterdam: A.A. Balkema.
- Madabhushi, S. P. G., Houghton, N. E., & Haigh, S. K. (2006). A new automatic sand pourer for model preparation at University of Cambridge. In *Proceedings of the 6th International Conference on Physical Modelling in Geotechnics* (pp. 217–222). London: Taylor & Francis.
- Madabhushi, S. S. C., Haigh, S. K., & Madabhushi, S. P. G. (2017). LEAP-GWU-2015: Centrifuge and numerical modelling of slope liquefaction at the University of Cambridge. *Soil Dynamics and Earthquake Engineering*. <https://doi.org/10.1016/j.soildyn.2016.11.009>
- Okamura, M., & Soga, Y. (2006). Effects of pore fluid compressibility on liquefaction resistance of partially saturated sand. *Soils and Foundations*, 46(5), 695–700.
- Schofield, A. N. (1981). Dynamic and earthquake geotechnical centrifuge modelling. *International Conferences on Recent Advances in Geotechnical Earthquake Engineering and Soil Dynamics*.
- Stringer, M. E., & Madabhushi, S. P. G. (2009). Novel computer-controlled saturation of dynamic centrifuge models using high viscosity fluids. *Geotechnical Testing Journal*, 32(6), 559–564.

**Open Access** This chapter is licensed under the terms of the Creative Commons Attribution 4.0 International License (<http://creativecommons.org/licenses/by/4.0/>), which permits use, sharing, adaptation, distribution and reproduction in any medium or format, as long as you give appropriate credit to the original author(s) and the source, provide a link to the Creative Commons license and indicate if changes were made.

The images or other third party material in this chapter are included in the chapter's Creative Commons license, unless indicated otherwise in a credit line to the material. If material is not included in the chapter's Creative Commons license and your intended use is not permitted by statutory regulation or exceeds the permitted use, you will need to obtain permission directly from the copyright holder.

